International Journal of Solids and Structures 45 (2008) 5368–5380

Contents lists available at ScienceDirect

International Journal of Solids and Structures

journal homepage: www.elsevier.com/locate/ijsolstr

High-frequency antiplane wave propagation in ultra-thin films with nanostructures

G.L. Huang [a,b,*], F. Song [b]

[a] Department of Systems Engineering, University of Arkansas at Little Rock, 2801 S University Ave, Little Rock, AR 72204, United States
[b] Department of Applied Science, University of Arkansas at Little Rock, Little Rock, AR 72204, United States

ARTICLE INFO

Article history:
Received 18 December 2007
Received in revised form 7 May 2008
Available online 10 June 2008

Keywords:
Continuum model
Wave propagation
Ultra-thin films
Nanostructural effects

ABSTRACT

Ultrasonic wave propagation is one of powerful and popular methods for measuring mechanical properties of solids even at nano scales. The extraction of material constants from the measured wave data may not be accurate and reliable when waves of short wavelengths are used. The objective of this paper is to study the high-frequency antiplane wave propagation in ultra-thin films at nanoscale. A developed continuum microstructure theory will be used to capture the effect of nanostructures in ultra-thin films. This continuum theory is developed from assumed displacement fields for nanostructures. Local kinematic variables are introduced to express these local displacements and are subjected to internal continuity conditions. The accuracy of the theory is verified by comparing the results with those of the lattice model for the antiplane problem in an infinite elastic medium. Specifically, dispersion curves and corresponding displacement fields for antiplane wave propagation in the ultra-thin films are studied. The inadequacy of the conventional continuum theory is discussed.

1. Introduction

Thin film science has grown world-wide into a major research area; specifically, ultra-thin, plate- or beam-like structures with submicron or nano thicknesses have attracted much attention due to their potential as highly sensitive, high-frequency devices for applications in microelectromechanical systems (MEMS) and nanoelectromechanical systems (NEMS) (Craighead, 2000; Yoon et al., 2005). As dimensions of the material become smaller, their resistance to deformation is increasingly determined by internal or external discontinuities (such as surfaces, grain boundary, strain gradient, and dislocation). For long-term reliability of various devices at nanoscale, researchers should understand the mechanical properties of ultra-thin films, especially for dynamic properties. Recently, growing interest of ultra-thin films in terahertz (THz) physics of nanoscale materials and integrated nano-photonic or nano-phononic devices (Vollmann et al., 2002, 2004; Ramprasad and Shi, 2005; Cai and Wang, 2006; Sampathkumar et al., 2006) opens a new topic on the wave characteristics of nanomaterials. Although many sophisticated approaches for predicting the mechanical properties of thin films exist, none keep up with the challenges posed by interior nanostructures such as the surfaces, interfaces, structural discontinuities and deformation gradient of the ultra-thin films under extreme loading conditions. The use of atomistic simulation may be a potential solution in the long run. However, it is well known the capability of this approach is limited by its need of prohibitive computing time and an astronomical amount of data generated in the calculations.

* Corresponding author. Address: Department of Systems Engineering, University of Arkansas at Little Rock, 2801 S University Ave, Little Rock, AR 72204, United States. Tel.: +1 501 683 7522; fax: +1 501 569 8698.
E-mail address: glhuang@ualr.edu (G.L. Huang).

0020-7683/$ - see front matter © 2008 Elsevier Ltd. All rights reserved.
doi:10.1016/j.ijsolstr.2008.05.033

It has been recognized that classical continuum models could not be adequate in describing the response of solids when the characteristic length (or wave length) of deformation becomes comparable to or smaller than the characteristic length of microstructures in the solid. Starting from Cosserat's model (1909), there have been different versions of continuum theories with microstructures proposed by different authors (Toupin, 1962; Mindlin, 1964; Eringen and Suhubi, 1964). In these theories, special kinematic variables were introduced to describe the local motion of microstructures. However, the large number of material constants were left undetermined, which would require rather prohibitive experiments. Recently, Chen et al. (2003) and Chen and Lee (2003a,b) have attempted to determine the material constants in the micromorphic theory (Eringen, 1999) by relating the micromorphic theory to atomistic models.

Another approach toward developing a continuum theory was taken by considering the exact configurations of the local structure in the system. By employing several kinematic variables to describe the local motion in addition to the macro kinematic variables, continuum models with micro- or nano-structures were derived (Sun et al., 1968; Achenbach et al., 1968; Huang and Sun, 2006) for periodically layered and nanostructure systems. The main advantage of this approach is that the material constants in the resulting continuum model are obtained directly from the original material system without ambiguity. Muhlhaus and Oka (1996) developed a continuum theory by direct homogenization of the discrete equations of motion for granular materials. The approach adopted was to simply replace finite differences by the corresponding Taylor expansion. In this analysis, the discrete system is considered as the identical masspoint connected to each other by non-linear elastic springs. Frieseche and James (2000) proposed a scheme from atomic level to continuum model. This model is based on the affine deformation of atoms to build passage from atomic level to continuum level, and is suitable for only static cases. Wang and Sun (2002) have introduced a continuum model with micro inertia that retains the simplicity of the classical continuum mechanics while capturing the characteristics of the microstructure. Compared with many studies in in-plane wave propagation in the nanostructural medium, much less attention has been paid to antiplane wave propagation. However, it should be mentioned that for many ultra-thin films' application, the antiplane wave propagation in those structures is one of fundamental issues in designing and predicting performance of micro- or nano-devices.

In the paper, a continuum model with nanostructures will be employed to study high-frequency antiplanewave propagation in ultra-thin films. The atomistic crystal structure of the ultra-thin film, for the sake of simplicity, is represented by a cubic lattice model. The dimensions of the crystal structure naturally appear in the constitutive equations and the equations of motion of the representative continuum. The accuracy of the present model is evaluated by comparing dispersions of free harmonic waves predicted by the continuum model and exact analysis based on the lattice model. Finally, the corresponding displacement fields in the nano-thin films are also investigated and discussed.

2. Microstructure continuum model for the ultra-thin film

A thin film of cubic structure is considered here as shown in Fig. 1. The thin film has a uniform thickness h and is assumed to be in a state of antiplane problem. Therefore, only displacement U_2 along X_2-direction is considered. The discrete solid dots denote atoms m_1 and m_2. The spacing between two adjacent atoms is a. Although the cubic structure is chosen for the sake of mathematical simplicity, the proposed approach can be readily applied for ultra-thin films with other crystal structures.

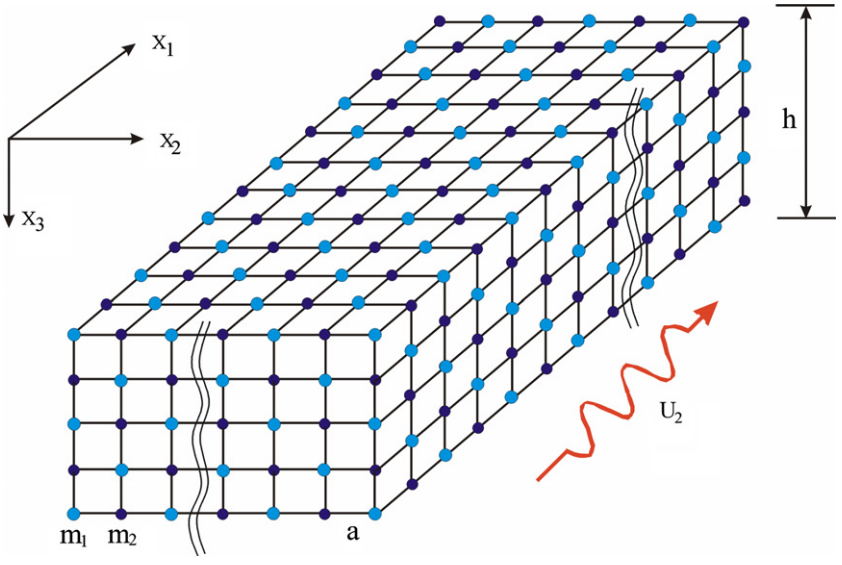

Fig. 1. Thin film structure and its lattice system.

2.1. Atomistic constitutive modeling

We consider the crystallite body consisting of N_0 atoms, as shown in Fig. 1. The kinematics are represented by the distance vectors between two atoms labeled i and j in the spatial and the material configuration:

$$ {}_{i-j}\vec{r} = {}_{i}\vec{r} - {}_{j}\vec{r} \quad \text{with} \quad {}_{i-j}r = |{}_{i-j}\vec{r}| \tag{1} $$

and

$$ {}_{i-j}\vec{R} = {}_{i}\vec{R} - {}_{j}\vec{R} \tag{2} $$

where ${}_{i}\vec{r}$ and ${}_{i}\vec{R}$ represent the spatial and the material position vectors at atom i. The displacements between atoms i and j are thus obtained as

$$ {}_{i-j}\vec{u} = {}_{i}\vec{u} - {}_{j}\vec{u} = {}_{i-j}\vec{r} - {}_{i-j}\vec{R} \tag{3} $$

There are many well-known empirical energy functions describing the inter-atom interaction. In their simplest form these empirical potentials contain only pair-wise interaction. The well known examples for this type of pair potentials include Morse, Buckingham and Lennard-Jones potentials, which are functions of only the relative scalar distance $r = {}_{i-j}r = |{}_{i-j}\vec{r}| = \sqrt{r_1^2 + r_2^2 + r_3^2}$ between two atoms. r_1, r_2 and r_3 are the vector $\vec{r}$ components along X_1, X_2 and X_3 directions. For example, the Lennard-Jones potential used as a prototype model in the work has the format

$$ V(r) = 4\varepsilon\left[\left(\frac{\sigma}{r}\right)^{12} - \left(\frac{\sigma}{r}\right)^{6}\right] \tag{4} $$

with ε denoting the strength of the interaction and σ denoting a characteristic length scale.

The potential energy of the atom i can be represented as sum over pair-wise interactions of this atom with all other atoms in the body

$$ {}_{i}V = \frac{1}{2}\sum_{j\neq i} V({}_{i-j}r) \tag{5} $$

Replacing the actual positions by the use of Eq. (3), the above expression becomes

$$ {}_{i}V = \frac{1}{2}\sum_{j\neq i} V({}_{i-j}R + {}_{i-j}u) \tag{6} $$

For the dynamics of the system with the particles staying in the neighborhood of the equilibrium configuration, $u = {}_{i-j}u = |{}_{i-j}\vec{u}| \ll |{}_{i-j}\vec{R}| = {}_{i-j}R = R$ and a Taylor series expansion with only the first two leading terms in displacements is justified as

$$ {}_{i}V = V^0 + \frac{1}{2}\sum_{j\neq i} V'_{\alpha}({}_{i-j}R)\,{}_{i-j}u_{\alpha} + \frac{1}{4}\sum_{j\neq i, m\neq n} V''_{\alpha\beta}({}_{i-j}R, {}_{m-n}R)({}_{i-j}u_{\alpha})({}_{m-n}u_{\beta}) \tag{7} $$

where

$$ V^0 = V(r)|_{r=R} $$

$$ V'_{\alpha}({}_{i-j}R) = \left.\frac{\partial V(r)}{\partial r_{\alpha}}\right|_{r=R} $$

$$ V''_{\alpha\beta}({}_{i-j}R, {}_{m-n}R) = \left.\frac{\partial^2 V(r)}{\partial r_{\alpha}\partial r_{\beta}}\right|_{r=R} $$

In the notation above, subscripts $\alpha, \beta = 1, 2, 3$ represent the components of the vector $\vec{r}$, V^0 is the potential energy corresponding to the equilibrium configuration, the coefficient $V'_{\alpha}({}_{i-j}R)$ is zero since the potential energy is minimum when atoms are in their equilibrium positions. Therefore, the deformation energy can be defined by

$$ {}_{i}W = {}_{i}V - V^0 = \frac{1}{4}\sum_{j\neq i, m\neq n} V''_{\alpha\beta}({}_{i-j}R, {}_{m-n}R)({}_{i-j}u_{\alpha})({}_{m-n}u_{\beta}) \tag{8} $$

If ${}_{i}F_{\alpha}$ denotes the force acting on the ith atom, then it will be given by

$$ {}_{i}F_{\alpha} = -\frac{\partial_i W}{\partial_i u_{\alpha}} = -\frac{1}{2}V''_{\alpha\alpha}({}_{i-j}R)\frac{\partial}{\partial_i u_{\alpha}}[{}_{i}u_{\alpha} - {}_{j}u_{\alpha}]^2 \tag{9} $$

For the antiplane problem with only non-trivial displacement component u_2, motion of atoms in any layer perpendicular to X_2-axis represents motion of the crystallite system. Therefore, for a specific in-plane layer in this cubic crystallite system, the location of an arbitrary ith atom in the layer at $X_1 = pa$ and $X_3 = qa$ can be denoted by (X_1^{pa}, X_3^{qa}). The displacement of the ith

atom in the layer is denoted by ${}_iu_2 = u_2^{(p,q)}$. The displacement of jth atoms near the ith atom can be represented as ${}_ju_2 = u_2^{(p\pm l,q\pm l)}$ with $l = 0, 1$. If we consider the force acting on the ith atom from the jth atoms with $R = a$ spacing is the nearest interaction and the force from the jth atoms with $R = \sqrt{2}a$ spacing is the next nearest interaction, we have the force acting on the ith atom as following:

$$\begin{aligned} {}_iF_\alpha = &-V''_{22}(a)\left[4u_2^{(p,q)} - u_2^{(p+1,q)} - u_2^{(p-1,q)} - u_2^{(p,q+1)} - u_2^{(p,q-1)}\right] \\ &- V''_{22}(\sqrt{2}a)\left[4u_2^{(p,q)} - u_2^{(p+1,q+1)} - u_2^{(p-1,q-1)} - u_2^{(p+1,q-1)} - u_2^{(p-1,q+1)}\right] \end{aligned} \tag{10}$$

From the Eq. (10), we find that $V''_{22}(a)$ and $V''_{22}(\sqrt{2}a)$ plays the role of the force constant, therefore the atomic stiffness of the near interaction and the next nearest interaction can be represented by linear elastic springs with spring constants as $\alpha_1 = V''_{22}(a)$ and $\alpha_2 = V''_{22}(\sqrt{2}a)$, respectively.

2.2. Microstructure continuum model

To consider small antiplane deformation in the discrete system, a representative unit cell of the cubic lattice model is considered, as shown in Fig. 2. In the study, only interactions between the nearest and next-nearest neighbors are considered, which are represented by linearly elastic springs with spring constants α_1 and α_2, respectively (Ghatak and Kothari, 1972). Compared with the simulation with real atomistic potential between atoms, this model is the first-order approximation at a small strain condition. It should be noted that the springs in Fig. 2 are the translational shear springs due to the shear deformation along X_2-direction. The representative cell consists of four sub-cells. In each sub-cell, a local coordinate system is established. Note that in this representative element, atoms 3, 6, 7, 8, and 9 are not included in the representative cell since they are included in the adjacent cells. The four local coordinate systems $(x_1^{(k)}, x_2^{(k)}, x_3^{(k)})$ with origins located at the geometrical centers of the four sub-cells k = 1–4, respectively, are set up so that x_1, x_2 and x_3 are parallel to the global (macro) coordinates X_1, X_2 and X_3, respectively.

The local antiplane displacements $u_2^{(k)}$ in the four subregions in the unit cell can be expanded in power series with respect to the respective local coordinates as

$$u_2^{(k)} = u_{02}^{(k)} + \phi_{12}^{(k)} x_1^{(k)} + \phi_{32}^{(k)} x_3^{(k)}, \quad k = 1, 2, 3, 4 \tag{11}$$

where the expansion is approximated by being truncated at the linear terms. The accuracy can be improved by involving higher order terms in Eq. (11). For the antiplane problem, we also have

$$u_1^{(k)} = u_3^{(k)} = 0 \tag{12}$$

It is assumed that local displacement $u_{02}^{(k)}$ of the four sub-cells are values of macrodisplacement U_2 at four sub-cells, respectively, i.e.

$$\begin{aligned} u_{02}^{(1)}(X_1, X_3) &= U_2(X_1, X_3) \\ u_{02}^{(2)} &\approx U_2(X_1 + a, X_3) \approx U_2(X_1, X_3) + a\frac{\partial U_2}{\partial X_1} \\ u_{02}^{(3)} &\approx U_2(X_1, X_3 + a) \approx U_2(X_1, X_3) + a\frac{\partial U_2}{\partial X_3} \\ u_{02}^{(4)} &\approx U_2(X_1 + a, X_3 + a) \approx U_2(X_1, X_3) + a\frac{\partial U_2}{\partial X_1} + a\frac{\partial U_2}{\partial X_3} \end{aligned} \tag{13}$$

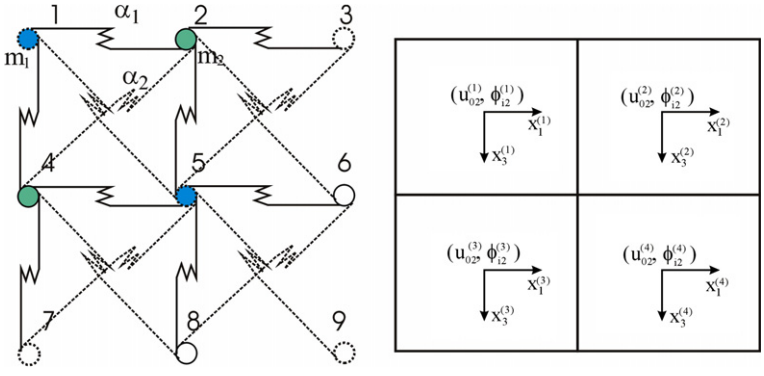

Fig. 2. Representative unit cell and the equivalent continuum.

The kinematic variables $u_{02}^{(k)}, \phi_{i2}^{(k)} (i = 1, 3)$ are required to satisfy the displacement continuity conditions along the boundaries shared by the adjacent pairs of the sub-cells. These boundary conditions lead to the following results:

$$\begin{Bmatrix} \phi_{12}^{(2)} \\ \phi_{32}^{(2)} \end{Bmatrix} = \begin{Bmatrix} 2\frac{\partial U_2}{\partial X_1} - \Phi_{12} \\ \Phi_{32} \end{Bmatrix} \tag{14}$$

$$\begin{Bmatrix} \phi_{12}^{(3)} \\ \phi_{32}^{(3)} \end{Bmatrix} = \begin{Bmatrix} \Phi_{12} \\ 2\frac{\partial U_2}{\partial X_3} - \Phi_{32} \end{Bmatrix} \tag{15}$$

$$\begin{Bmatrix} \phi_{12}^{(4)} \\ \phi_{32}^{(4)} \end{Bmatrix} = \begin{Bmatrix} 2\frac{\partial U_2}{\partial X_1} - \Phi_{12} \\ 2\frac{\partial U_2}{\partial X_3} - \Phi_{32} \end{Bmatrix} \tag{16}$$

in which

$$\Phi_{i2}(X_1, X_3) \equiv \phi_{i2}^{(1)}(X_1, X_3), \quad i = 1, 3 \tag{17}$$

The deformation energy in each sub-cell can be expressed as

$$W^{(1)} = W_{1-2} + W_{1-4} + W_{1-5} + W_{2-4} \tag{18}$$

$$W^{(2)} = W_{2-3} + W_{2-5} + W_{2-6} + W_{3-5} \tag{19}$$

$$W^{(3)} = W_{4-5} + W_{4-7} + W_{4-8} + W_{5-7} \tag{20}$$

$$W^{(4)} = W_{5-6} + W_{5-8} + W_{5-9} + W_{6-8} \tag{21}$$

where superscripts 1, 2, 3, 4 represent the sub-cells, and $W_{1-2}, W_{1-5} \ldots$ denote the total deformation energies due to antiplane deformation of the springs between atoms 1 and 2 and 1 and 5…, respectively. Detailed derivations for W_{1-2} and W_{1-5} are presented in the following to illustrate the procedure. Other terms can be determined in a similar method.

Consider the deformation energy W_{1-2} between atoms 1 and 2. The displacements of atom 2 can be obtained from sub-cell 1 or sub-cell 2. For simplicity, the displacements for atoms 1 and 2 are both taken from sub-cell 1. We have

$$W_{1-2} = \frac{1}{2}\alpha_1({}_2u_2^{(1)} - {}_1u_2^{(1)})^2 = \frac{1}{2}\alpha_1(a\phi_{12}^{(1)})^2 \tag{22}$$

where ${}_su_2^{(k)}$ represents displacement component u_2 in the sub-cell k at atom s.

Likewise, the deformation energy between atoms 1 and 5 can be expressed as

$$W_{1-5} = \frac{1}{2}\alpha_2({}_5u_2^{(1)} - {}_1u_2^{(1)})^2 = \frac{1}{2}\alpha_2(a\phi_{12}^{(1)} + a\phi_{32}^{(1)})^2 \tag{23}$$

The total deformation energy in sub-cell 1 is

$$W^{(1)} = \frac{1}{2}(\alpha_1 + 2\alpha_2)a^2[(\phi_{12}^{(1)})^2 + (\phi_{32}^{(1)})^2] \tag{24}$$

The deformation energies for other sub-cells have a similar expression as Eq. (24). Based on Eqs. (14)–(16), the kinematic variables $\phi_{i2}^{(k)} (k = 2, 3, 4)$ in sub-cells 2, 3, and 4 can be eliminated and expressed in terms of the kinematic variables of sub-cell 1. Therefore, the total deformation energy in the representative unit cell can be expressed in terms of U_2, Φ_{i2} and their derivatives. By dividing this total energy with the planar area $4a^2$, we obtain the deformation energy density W of the representative cell after some manipulations. We have

$$W = \frac{1}{4a^2}\left(W^{(1)} + W^{(2)} + W^{(3)} + W^{(4)}\right) = \frac{1}{2}(\alpha_1 + 2\alpha_2)(E_{12}^2 + E_{32}^2 + \gamma_{12}^2 + \gamma_{32}^2) \tag{25}$$

in which

$$E_{i2} = U_{2,i}, \quad i = 1, 3 \tag{26}$$

is the macrostrain and

$$\gamma_{i2} = U_{2,i} - \Phi_{i2}, \quad i = 1, 3 \tag{27}$$

is the relative strain. These two deformation variables resemble those in Mindlin's microstructure theory (Mindlin, 1964). This deformation energy function forms the base of the continuum model that represents the discrete lattice system.

Based on the total deformation energy density, the corresponding Cauthy stresses and the relative stresses can be obtained by

$$\Sigma_{i2} = \frac{\partial W}{\partial E_{i2}} = (\alpha_1 + 2\alpha_2)E_{i2} \tag{28}$$

and

$$\sigma_{i2}^{\mathrm{R}} = \frac{\partial W}{\partial \gamma_{i2}} = (\alpha_1 + 2\alpha_2)\gamma_{i2} \tag{29}$$

It is noted that the relative stress σ_{i2}^{R} vanishes if γ_{i2} is absent and the deformation energy density function reduces to that of the classical continuum. This reduced model will be referred to as the "effective modulus" theory.

The kinetic energy density function for the representative cell can be derived from the discrete system based on the local displacements given by Eq. (11). We obtain

$$T = \frac{m_1}{4a^2}\left[\dot{U}_2^2 + \frac{a^2}{4}(\dot{\Phi}_{12} + \dot{\Phi}_{32})^2\right] + \frac{m_2}{4a^2}\left[\dot{U}_2^2 + \frac{a^2}{4}(\dot{\Phi}_{12} - \dot{\Phi}_{32})^2\right] \tag{30}$$

where a dot represents the derivative with respect to time t.

To complete the continuum model, we derive the equations of motion and boundary conditions by the Hamilton's principle. Let A be a region of the thin film represented by the continuum model. Then the Hamilton's principle states

$$\delta \int_{t_0}^{t_1} \int_A (T - W)\mathrm{d}V\mathrm{d}t + \int_{t_0}^{t_1} \int_S (T_i \delta U_i + P_{ji}\delta \Phi_{ji})\mathrm{d}A\mathrm{d}t = 0 \tag{31}$$

in which S is the entire boundary of A, T_i is external traction, and P_{ji} the external couple applied along S. Substituting Eqs. (25) and (30) in Eq. (31) and perform variations, we obtain the equations of motion:

$$-\frac{1}{2a^2}(m_1 + m_2)\ddot{U}_2 + (\alpha_1 + 2\alpha_2)\left(2\frac{\partial^2 U_2}{\partial X_1^2} + 2\frac{\partial^2 U_2}{\partial X_3^2} - \frac{\partial \Phi_{12}}{\partial X_1} - \frac{\partial \Phi_{32}}{\partial X_3}\right) = 0 \tag{32}$$

$$\frac{1}{8}(m_1 + m_2)\ddot{\Phi}_{12} + \frac{1}{8}(m_1 - m_2)\ddot{\Phi}_{32} + (\alpha_1 + 2\alpha_2)\left(\Phi_{12} - \frac{\partial U_2}{\partial X_1}\right) = 0 \tag{33}$$

$$\frac{1}{8}(m_1 + m_2)\ddot{\Phi}_{32} + \frac{1}{8}(m_1 - m_2)\ddot{\Phi}_{12} + (\alpha_1 + 2\alpha_2)\left(\Phi_{32} - \frac{\partial U_2}{\partial X_3}\right) = 0 \tag{34}$$

The boundary conditions are

$$T_2 = (\Sigma_{i2} + \sigma_{i2}^R)n_i, \quad P_{ji} = 0 \tag{35}$$

where n_i is the unit vector normal to the boundary surface. It is noted that, for the present continuum model developed based on the linear displacement expansion of Eq. (11), no couple stress is present.

The equations of motion for the reduced effective modulus theory are readily obtained by requiring $\gamma_{i2} = 0$ in the energy density function. We have

$$(\alpha_1 + 2\alpha_2)\left(\frac{\partial^2 U_2}{\partial X_1^2} + \frac{\partial^2 U_2}{\partial X_3^2}\right) = \frac{1}{2a^2}(m_1 + m_2)\ddot{U}_2 \tag{36}$$

3. Antiplane wave propagation in an infinite lattice system

To validate the present continuum model, we first consider harmonic antiplane wave propagation in an infinite lattice system by using both the exact solution and the current microstructure continuum model.

The lattice is assumed to be infinite extent in all three dimensions. The microstructure of the lattice is shown in Fig. 1, where X_1 and X_3-directions are defined as in-plane directions and X_2-direction is defined as antiplane direction. For the infinite lattice system, the thickness of the lattice system h is assumed to be infinite.

3.1. Exact solution of wave propagation

For the antiplane problem with only non-trivial displacement component u_2, motion of atoms in any layer perpendicular to X_2-axis represents motion of the lattice system. The X_1 and X_3-directions are defined as in-plane directions and the X_2-direction is defined as antiplane direction. Therefore, for a specific in-plane layer, the location of an arbitrary atom in the layer at $X_1 = pa$ and $X_3 = qa$ can be denoted by (X_1^{pa}, X_3^{qa}). The displacement of the atom in the layer is denoted by $u_2^{(p,q)}$.

For the unit cell of atoms at $X_1 = ia$ and $X_3 = ja$ and $X_1 = ia$ and $X_3 = (j+1)a$, the equations of motion can be written as

$$m_1\ddot{u}_2^{(i,j)} = -\alpha_1\left(4u_2^{(i,j)} - u_2^{(i,j+1)} - u_2^{(i,j-1)} - u_2^{(i+1,j)} - u_2^{(i-1,j)}\right) - \alpha_2\left(4u_2^{(i,j)} - u_2^{(i+1,j+1)} - u_2^{(i-1,j-1)} - u_2^{(i+1,j-1)} - u_2^{(i-1,j+1)}\right) \tag{37}$$

$$m_2\ddot{u}_2^{(i,j+1)} = -\alpha_1\left(4u_2^{(i,j+1)} - u_2^{(i,j+2)} - u_2^{(i,j)} - u_2^{(i+1,j+1)} - u_2^{(i-1,j+1)}\right) - \alpha_2\left(4u_2^{(i,j+1)} - u_2^{(i+1,j+2)} - u_2^{(i-1,j)} - u_2^{(i+1,j)} - u_2^{(i-1,j+2)}\right) \tag{38}$$

where the mass of the atom at $X_1 = ia$ and $X_3 = ja$ is assumed to be m_1, and the mass of the atom at $X_1 = ia$ and $X_3 = (j+1)a$ is assumed to be m_2.

The harmonic antiplane wave along X_1-direction assumes the form

$$u_2^{(p,q)} = A_1 e^{ik(X_1^p - ct)} \quad \text{for the atom} \quad m_1 \tag{39}$$

$$u_2^{(p,q+1)} = A_2 e^{ik(X_1^p - ct)} \quad \text{for the atom} \quad m_2 \tag{40}$$

where $X_1^p = pa$.

Substituting Eqs. (39) and (40) in Eqs. (37) and (38), we obtain

$$(m_1\omega^2 - 4\alpha_1 - 4\alpha_2 + 4\alpha_2\cos(ka))A_1 + (2\alpha_1 + 2\alpha_1\cos(ka))A_2 = 0 \tag{41}$$

$$(2\alpha_1 + 2\alpha_1\cos(ka))A_1 + (m_2\omega^2 - 4\alpha_1 - 4\alpha_2 + 4\alpha_2\cos(ka))A_2 = 0 \tag{42}$$

The dispersion equation can be obtained by requiring that the determinant of the coefficient matrix vanishes.

3.2. Continuum model of wave propagation

The microstructure continuum theory presented in Section 2 is now employed to study propagation of antiplane harmonic waves in the infinite lattice system. Harmonic waves propagating in the X_1-direction can be expressed as

$$U_2 = \overline{A} e^{ik(X_1 - ct)}, \tag{43}$$

$$\Phi_{12} = \overline{B} e^{ik(X_1 - ct)}, \tag{44}$$

$$\Phi_{32} = \overline{C} e^{ik(X_1 - ct)}, \tag{45}$$

where k denotes wave number, c is phase velocity, and $\overline{A}, \overline{B}, \overline{C}$ are unknown constants independent of the macro coordinates X_1, X_2 and X_3. Substituting Eqs. (43)–(45) in equations of motion (32)–(34), we obtain

$$\left[-\frac{\omega^2}{2a^2}(m_1 + m_2) + 2(\alpha_1 + 2\alpha_2)k^2\right]\overline{A} + (\alpha_1 + 2\alpha_2)ik\overline{B} = 0 \tag{46}$$

$$(\alpha_1 + 2\alpha_2)ik\overline{A} + \left[\frac{1}{8}(m_1 + m_2)\omega^2 - (\alpha_1 + 2\alpha_2)\right]\overline{B} + \frac{1}{8}(m_1 - m_2)\omega^2\overline{C} = 0 \tag{47}$$

$$\left[\frac{1}{8}(m_1 - m_2)\omega^2\right]\overline{B} + \left[\frac{1}{8}(m_1 + m_2)\omega^2 - (\alpha_1 + 2\alpha_2)\right]\overline{C} = 0 \tag{48}$$

where $\omega = kc$ denotes the circular frequency.

Eqs. (46)–(48), have non-trivial solutions for $\overline{A}, \overline{B}, \overline{C}$ only if the determinant of the coefficients vanishes. This results in the dispersion equation:

$$\begin{vmatrix} H_1 & H_2 & 0 \\ H_2 & H_3 & H_4 \\ 0 & H_4 & H_3 \end{vmatrix} = 0 \tag{49}$$

where

$$H_1 = -\frac{\omega^2}{2a^2}(m_1 + m_2) + 2(\alpha_1 + 2\alpha_2)k^2$$

$$H_2 = (\alpha_1 + 2\alpha_2)ik$$

$$H_3 = \frac{1}{8}(m_1 + m_2)\omega^2 - (\alpha_1 + 2\alpha_2)$$

$$H_4 = \frac{1}{8}(m_1 - m_2)\omega^2$$

4. Antiplane wave propagation in the ultra-thin film

We now consider harmonic antiplane wave propagation in a plate lattice system, as shown in Fig. 1. Similarly, the X_1 and X_3-directions are defined as in-plane directions and the X_2-direction is defined as antiplane direction. The coordinate system is established so that the X_1-axis coincides with the top boundary layer of atoms and X_3-axis coincides with an arbitrary column of atoms. The nanoplate is assumed to consist of $N + 1$ atom layers with thickness h in the X_3-direction. Both the exact solution and the continuum model will be used for the simulation of wave propagation.

4.1. Exact solution of wave propagation

Consider the ith column of atoms at $X_1 = ia$. The equation of motion for the atom at the top layer ($X_3 = 0$) can be expressed as

$$m_1\ddot{u}_2^{(i,0)} = -\alpha_1(3u_2^{(i,0)} - u_2^{(i,1)} - u_2^{(i+1,0)} - u_2^{(i-1,0)}) - \alpha_2(2u_2^{(i,0)} - u_2^{(i+1,1)} - u_2^{(i-1,1)}) \tag{50}$$

in which the mass of the atom at the top layer is assumed to be m_1. Similarly, the equation of motion for the atom at the bottom layer ($X_3 = Na$) is

$$m_1\ddot{u}_2^{(i,N)} = -\alpha_1(3u_2^{(i,N)} - u_2^{(i,N-1)} - u_2^{(i+1,N)} - u_2^{(i-1,N)}) - \alpha_2(2u_2^{(i,N)} - u_2^{(i-1,N-1)} - u_2^{(i+1,N-1)}) \tag{51}$$

where the mass of the atom at the bottom layer is also assumed to be m_1 in order to make the lattice system symmetric with respect to its mid-plane.

The equations of motion for the interior atoms in the ith column are

$$m\ddot{u}_2^{(i,j)} = -\alpha_1(4u_2^{(i,j)} - u_2^{(i,j+1)} - u_2^{(i,j-1)} - u_2^{(i+1,j)} - u_2^{(i-1,j)}) - \alpha_2(4u_2^{(i,j)} - u_2^{(i+1,j+1)} - u_2^{(i-1,j-1)} - u_2^{(i+1,j-1)} - u_2^{(i-1,j+1)}) \tag{52}$$

where $j = 1, 2, 3, \ldots, N-1$ and $m = m_1$ if j is an even number and $m = m_2$ otherwise.

For an antiplane harmonic wave propagating in the X_1-direction, the displacements can be assumed as

$$u_2^{(p,q)} = A^q e^{ik(X_1^p - ct)} \tag{53}$$

where $X_1^p = pa$. Substitution of Eq. (53) in Eqs. (50)–(52) yields $N+1$ equations for the unknown coefficients vector $A = \{A^0, A^1, \ldots, A^j, \ldots, A^N\}$. The dispersion equation is obtained by requiring that the determinant of the coefficient matrix vanishes. By solving the systems of equations mentioned above, we can get the corresponding displacement fields of respective atoms.

4.2. Continuum model of wave propagation in the thin film

The continuum model of antiplane harmonic waves in the thin film is studied in this subsection. The thickness of the thin film is assumed to be h. Harmonic waves propagating in the X_1-direction can be expressed as

$$U_2 = f_1(X_3)e^{ik(X_1 - ct)} \tag{54}$$

$$\Phi_{12} = f_2(X_3)e^{ik(X_1 - ct)} \tag{55}$$

$$\Phi_{32} = f_3(X_3)e^{ik(X_1 - ct)} \tag{56}$$

where $f_i(X_3)$ are unknown functions. Substituting Eqs. (54)–(56) in the equations of motion (32)–(34), we obtain

$$\left[\frac{1}{2a^2}(m_1 + m_2)\omega^2 - 2(\alpha_1 + 2\alpha_2)k^2\right]f_1 + 2(\alpha_1 + 2\alpha_2)f_1'' - (\alpha_1 + 2\alpha_2)ikf_2 - (\alpha_1 + 2\alpha_2)f_3' = 0 \tag{57}$$

$$(\alpha_1 + 2\alpha_2)ikf_1 + \left[\frac{1}{8}(m_1 + m_2)\omega^2 - (\alpha_1 + 2\alpha_2)\right]f_2 + \frac{1}{8}(m_1 - m_2)\omega^2 f_3 = 0 \tag{58}$$

$$(\alpha_1 + 2\alpha_2)f_1' + \frac{1}{8}(m_1 - m_2)\omega^2 f_2 + \left[\frac{1}{8}(m_1 + m_2)\omega^2 - (\alpha_1 + 2\alpha_2)\right]f_3 = 0 \tag{59}$$

where a prime indicates differentiation with respect to X_3. By eliminating f_2, f_3 from Eqs. (57)–(59), the following differential equation for f_1 can be obtained:

$$(C_1 + C_2)f_1'' - 2C_3 f_1' + (C_4 + C_5)f_1 = 0 \tag{60}$$

where

$$C_1 = 2(D_4^2 - D_5^2)D_2, \quad C_2 = D_2^2 D_4$$

$$C_3 = D_2 D_3 D_5, \quad C_4 = (D_4^2 - D_5^2)D_1, \quad C_5 = D_3^2 D_4$$

$$D_1 = \frac{1}{2a^2}(m_1 + m_2)\omega^2 - 2(\alpha_1 + 2\alpha_2)k^2, \quad D_2 = \alpha_1 + 2\alpha_2$$

$$D_3 = ik(\alpha_1 + 2\alpha_2), \quad D_4 = \frac{1}{8}(m_1 + m_2)\omega^2 - (\alpha_1 + 2\alpha_2), \quad D_5 = \frac{1}{8}(m_1 - m_2)\omega^2$$

The general solutions of Eq. (60) for the function f_1 depend on the type of the roots of characteristic equation

$$(C_1 + C_2)\beta^2 - 2C_3\beta + (C_4 + C_5) = 0 \tag{61}$$

By solving the above quadratic equation, the general solution for f_1 can be expressed as

$$f_1 = E_1 e^{\beta_1 X_3} + E_2 e^{\beta_2 X_3} \tag{62}$$

where β_1, β_2 are two roots of Eq. (61). The solutions for f_2, f_3 can be obtained in a similar way.

For this antiplane problem, the traction-free boundary conditions at $X_3 = 0$ and $X_3 = h$ lead to

$$S_1E_1 + S_2E_2 = 0 \tag{63}$$

$$S_1E_1e^{\beta_1 h} + S_2E_2e^{\beta_2 h} = 0 \tag{64}$$

where

$$S_1 = 2\beta_1 - \frac{D_2D_4\beta_1 - D_3D_5}{D_5^2 - D_4^2}, \quad S_2 = 2\beta_2 - \frac{D_2D_4\beta_2 - D_3D_5}{D_5^2 - D_4^2}$$

Eqs. (63) and (64) have non-trivial solutions for E_1, E_2 only when the determinant of the coefficients vanishes. This results in the dispersion equation:

$$\begin{vmatrix} S_1 & S_2 \\ S_1e^{\beta_1 h} & S_2e^{\beta_2 h} \end{vmatrix} = 0 \tag{65}$$

The corresponding displacement field (54) can be obtained by substituting the solutions in Eq. (65) into Eqs. (63) and (64) and solving the eigenvector equations.

5. Numerical simulation

This section concerns numerical simulation of antiplane wave propagation in the different lattice systems, discussed in Sections 3 and 4. It is well known that in a classical elastic solid, the antiplane wave is non-dispersive. However, antiplane waves with wavelengths that are comparable to the atomic spacing must be carefully examined if the wave technique is to be used in measuring material constants. It is noteworthy that, especially in electronic device applications, antiplane wave frequencies on the order of GHz–THz are now possible for this type of measurement.

5.1. Wave propagation in the infinite lattice system

For the current lattice system, there exist two modes of wave forms. The lower frequency one is the acoustic mode and the higher frequency one is the optical mode. For the acoustic mode, adjacent atoms move in the same direction (in phase), and for the optic mode, adjacent atoms move in the opposite direction (out of phase). Fig. 3 shows the comparison of dispersion curves for the acoustic mode obtained according to Eqs. (41) and (42) of the exact solution for the lattice systems, the microstructure continuum model (49), and the effective modulus theory (36), respectively. The parameters used in the calculation for the cubic structure are $a = 1.74 \times 10^{-10}$ m, $\alpha_1 = 2.02$ N/m, $\alpha_2 = 1.10$ N/m, and $m_2/m_1 = 10$. The non-dimensional wave velocity $c^* = c/\sqrt{\frac{\alpha_2}{\rho_0}}$, with $\rho_0 = \frac{m_1+m_2}{2a^2}$, and non-dimensional wave number ka are used in the figure. The results of Fig. 3 show that both the effective modulus theory and the microstructure continuum model yield very good predictions for the anti-symmetric wave for long waves with $ka < 0.2$. However, as wave length decreases, the dispersion curve computed

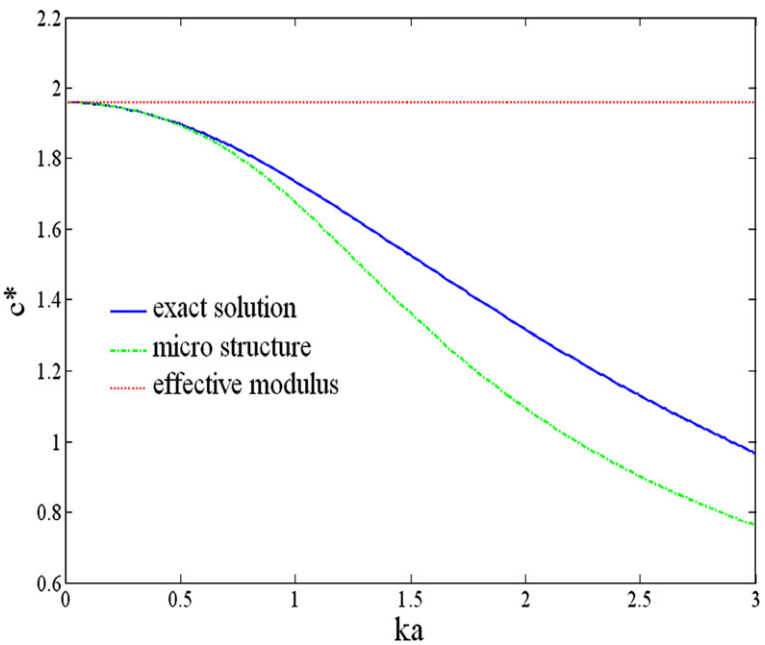

Fig. 3. Dispersion curves for the acoustic mode obtained by the lattice model and continuum model for an infinite medium.

from the effective modulus theory deviates substantially from the exact curve, while the curve predicted by the microstructure continuum model is in good agreement with the exact curve even when $ka = 1.0$. On the other hand if one employs the effective modulus theory and waves with $ka > 0.2$ to determine elastic constants of a thin film with the aid of the dispersion relations, the values of these constants may be significantly overestimated.

Fig. 4 shows the comparison of the non-dimensional angular frequency $\omega* = \omega/\omega_0$ for the optic mode with $\omega_0 = \frac{\sqrt{\alpha_2/\rho_0}}{2a}$. It is found that the microstructure continuum model can capture the trend of the phase velocity of the optic wave mode but the value of the phase velocity even for very low frequency cases. This discrepancy is attributed to the fact that only linear terms are considered in the local displacements. To better capture the properties of the higher order wave mode, higher order expansion terms in Eq. (11) and the correction factor coefficients must be added in the development of the continuum model. The detailed development of the higher order microstructure continuum model to capture the higher order wave mode can be found in a separate publication (Huang and Sun, in press).

5.2. Wave propagation in the plate lattice system

In the subsection, we will focus on the lowest wave mode (acoustic wave mode) for antiplane wave propagation in the plate lattice system. Fig. 5 shows the comparison of dispersion curves for the acoustic mode obtained by the exact solution for the nanoplate lattice systems, the microstructure continuum model, and the effective modulus theory, respectively. The parameters used in the computation for the cubic structure are $a = 1.74 \times 10^{-10}$ m, $\alpha_1 = 2.02$ N/m, $\alpha_2 = 1.10$ N/m, $m_2/m_1 = 10$ and $h = 8a$. It is expected that the dispersion curve predicted by the present microstructure continuum model shows better agreement with the exact solution than that by the effective modulus theory. However, it is of interest to note that the results by both the continuum theories and the effective modulus theory show some difference relative to the exact phase velocity even at long wave lengths. This discrepancy is attributed to the fact both the present continuum theory and the effective modulus theory are not capable of accounting for the nano scale surface effect on the thin film.

Fig. 6 shows comparisons of dispersion curves for the nanoplate lattice system of thickness $h = 20a$. Conclusions similar to those for the results of Fig. 5 can be made here except for phase velocities at long wave lengths, which are found to be in fairly good agreement with that of the exact lattice model. Consequently, if one wants to use the lowest antiplane wave mode to determine thin film material properties, some data corrections should be exercised when the thickness of the ultra-thin film is less than 6–7 nm.

Displacement fields will also provide the important information of the antiplane wave propagation, especially for the prediction of the wave motion shape in the ultra-thin films. Displacement fields can be obtained by solving the eigenvector problem for the lattice model and microstructure continuum model, respectively. Fig. 7 shows the comparison of the normalized antiplane displacement fields across the thickness in the ultra-thin film for the loading frequency $ka = 0.525$ by using the lattice model and microstructure continuum model. The material properties used in the calculations are $a = 1.74 \times 10^{-10}$ m, $\alpha_1 = 2.02$ N/m, $\alpha_2 = 1.10$ N/m, $m_2/m_1 = 10$ and $h = 40a$. The normalized amplitude A^* is defined as A/A_{mid}, where A_{mid} represents the amplitude of the displacement field in the middle of the thin film. As shown in Fig. 7,

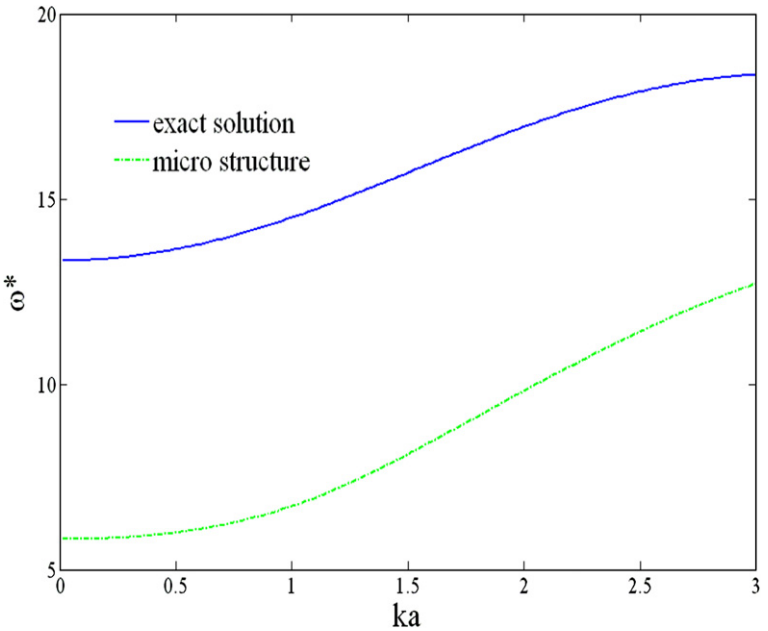

Fig. 4. Dispersion curves for the optic mode obtained by the lattice model and continuum model for an infinite medium.

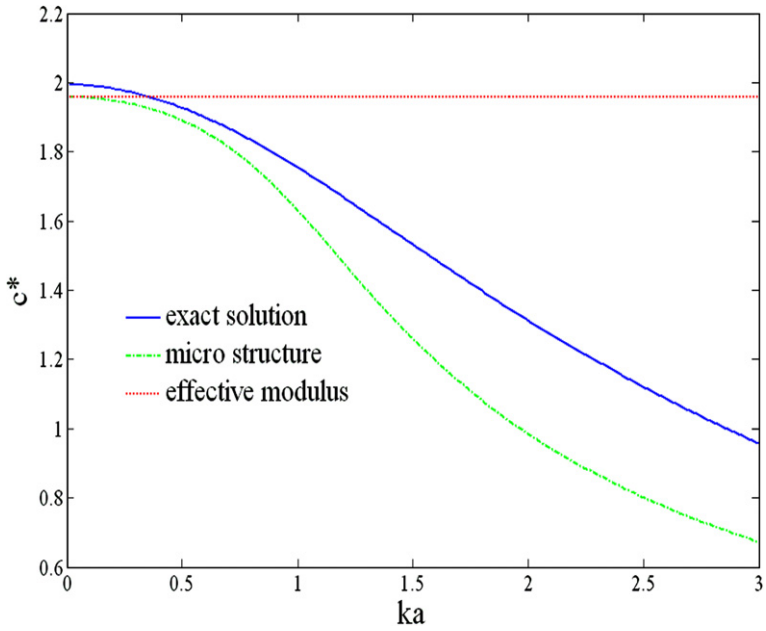

Fig. 5. Dispersion curves for the lowest antiplane wave mode obtained by the lattice model and continuum models for the thin film with eight atom layers.

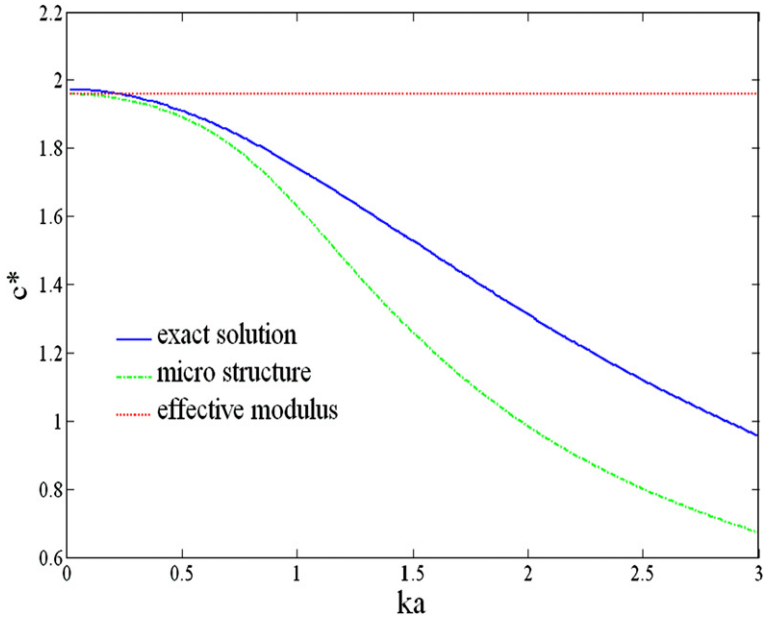

Fig. 6. Dispersion curves for the lowest antiplane wave mode obtained by the lattice model and continuum models for the ultra-thin film with 20 atom layers.

the displacement fields predicted by the lattice model are represented by two discontinuous curves. This is due to the mass difference in the lattice model. It can be also found that the current microstructure continuum model can still give very reasonable prediction about the displacement fields in the ultra-thin films.

6. Concluding remarks

In this paper, we have examined high-frequency harmonic antiplane wave propagation in ultra-thin films using the classical continuum (effective modulus) theory and a microstructure continuum theory. This microstructure continuum theory

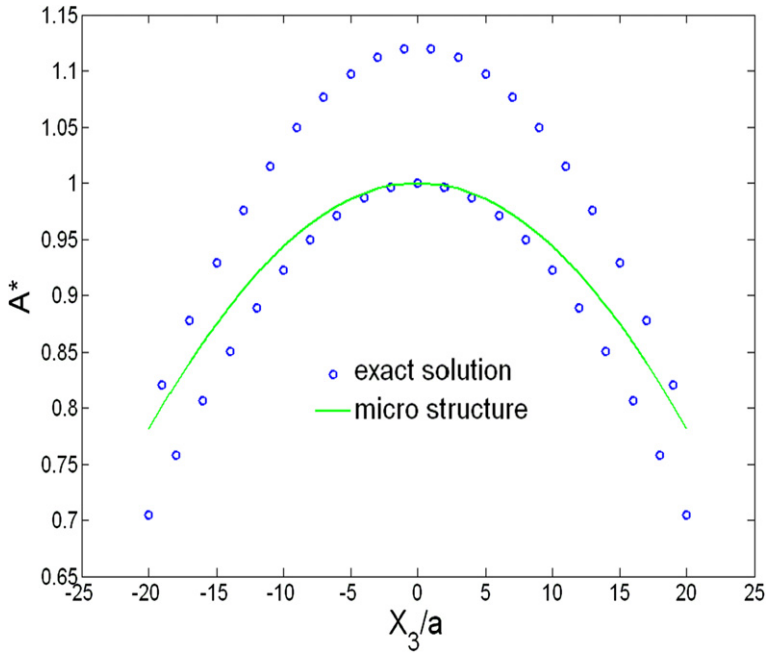

Fig. 7. Normalized displacement fields predicted by the lattice model and the microstructure continuum theory.

is developed by introducing local kinematic variables to express these local displacements. The accuracy of the theory is verified by comparing the results with those of the lattice model. It was found that the effective modulus theory is inadequate to describe waves of short wavelengths propagating in the ultra-thin films. However, the microstructure continuum theory can provide good predictions of both dispersive wave velocities and displacement fields, which is useful for the prediction of properties of nanomaterials. Based on the theory, further study of dynamic non-linear wave propagation in the nanostructured materials will be conducted by using the real atomistic potential.

Acknowledgements

This research was funded, in part, by the National Science Foundation EPSCoR Grant # EPS-0701890. Also, the authors are thankful to one of the reviewers of the paper for his/her helpful comments.

References

Achenbach, J.D., Sun, C.T., Herrmann, G., 1968. On the vibrations of a laminated body. ASME Journal of Applied Mechanics 35, 689–696.
Cai, H., Wang, X., 2006. Effect of initial stress on transverse wave propagation in carbon nanotubes based on Timoshenko laminated beam models. Nanotechnology 17, 45–53.
Chen, Y., Lee, J.D., 2003a. Connecting molecular dynamics to micromorphic theory. (I). Instantaneous and averaged mechanical variables. Physics A 322, 359–376.
Chen, Y., Lee, J.D., 2003b. Determining material constants in micromorphic theory through phonon dispersion relations. International Journal of Engineering Science 41, 871–886.
Chen, Y., Lee, J.D., Eskandarian, A., 2003. Atomistic counterpart of micromorphic theory. Acta Mechanica 161, 81–102.
Cosserat, E., Cosserat, F., 1909. Theorie des Corps Deformables, A. Hermann & Fils, Paris.
Craighead, H.G., 2000. Nanoelectromechanical system. Science 290, 1532–1535.
Eringen, A.C., 1999. Microcontinuum Field Theories. I. Foundations and Solids. Springer Verlag, New York.
Eringen, A.C., Suhubi, E.S., 1964. Nonlinear theory of micro-elastic solids. International Journal of Engineering Science 2, 189–203.
Frieseche, G., James, R.D., 2000. A scheme for the passage from atomic to continuum theory for thin films, nanotubes and nanorods. Journal of the Mechanics and Physics of Solids 48, 1519–1540.
Ghatak, A., Kothari, L., 1972. An Introduction to Lattice Dynamics. Addison-Wesley.
Huang, G.L., Sun, C.T., 2006. A continuum model with microstructure for wave propagation in ultra-thin films. International Journal of Solids and Structures 43, 7104–7127.
Huang, G.L., Sun, C.T., in press. Higher order continuum model for elastic media with multiphased microstructure. Mechanics of Advanced Materials and Structures.
Mindlin, R.D., 1964. Micro-structure in linear elasticity. Archive for Rational Mechanics and Analysis 16, 51–78.
Muhlhaus, H.B., Oka, F., 1996. Dispersion and wave propagation in discrete and continuous models for granular materials. International Journal of Solids and Structures 33, 2841–2858.
Ramprasad, R., Shi, N., 2005. Scalibility of phononic crystal heterostructures. Applied Physics Letters 87, 111101.
Sampathkumar, A., Murray, T.W., Ekinci, K.L., 2006. Photothermal operation of high frequency nanoelectromechanical systems. Applied Physics Letters 88, 223104.
Sun, C.T., Achenbach, J.D., Herrmann, G., 1968. Continuum theory for a laminated medium. ASME Journal of Applied Mechanics 35, 467–475.

Toupin, R.A., 1962. Elastic materials with couple-stresses. Archive for Rational Mechanics and Analysis 11, 385–414.
Vollmannn, J., Profunser, D.M., Dual, J., 2002. Sensitivity improvement of a pump-probe set-up for thin film and microstructure metrology. Ultrasonics 40, 757–763.
Vollmannn, J., Profunser, D.M., Meier, A.H., Dobeli, M., Dual, J., 2004. Pulse laser acoustics for the characterization of inhomogeneities at interfaces of microstructures. Ultrasonics 42, 657–663.
Wang, Z.P., Sun, C.T., 2002. Modeling micro-inertia in heterogeneous materials under dynamic loading. Wave Motion 36, 473–485.
Yoon, J., Ru, C.Q., Mioduchowski, A., 2005. Terahertz vibration of short carbon nanotubes modeled as Timoshenko beams. Transactions of the ASME Journal of Applied Mechanics 72, 10–17.